TU Delft

Delft University of Technology

Damping of Magnetization Dynamics by Phonon Pumping

Streib, Simon; Keshtgar, Hedyeh; Bauer, Gerrit E.W.

DOI
10.1103/PhysRevLett.121.027202

Publication date
2018

Document Version
Final published version

Published in
Physical Review Letters

Citation (APA)
Streib, S., Keshtgar, H., & Bauer, G. E. W. (2018). Damping of Magnetization Dynamics by Phonon Pumping. *Physical Review Letters*, *121*(2), Article 027202. https://doi.org/10.1103/PhysRevLett.121.027202

Important note
To cite this publication, please use the final published version (if applicable).
Please check the document version above.

Copyright
Other than for strictly personal use, it is not permitted to download, forward or distribute the text or part of it, without the consent of the author(s) and/or copyright holder(s), unless the work is under an open content license such as Creative Commons.

Takedown policy
Please contact us and provide details if you believe this document breaches copyrights.
We will remove access to the work immediately and investigate your claim.

This work is downloaded from Delft University of Technology.
For technical reasons the number of authors shown on this cover page is limited to a maximum of 10.

Damping of Magnetization Dynamics by Phonon Pumping

Simon Streib,[1] Hedyeh Keshtgar,[2] and Gerrit E. W. Bauer[1,3]
[1]Kavli Institute of NanoScience, Delft University of Technology, Lorentzweg 1, 2628 CJ Delft, Netherlands
[2]Institute for Advanced Studies in Basic Science, 45195 Zanjan, Iran
[3]Institute for Materials Research and WPI-AIMR and CSRN, Tohoku University, Sendai 980-8577, Japan

(Received 22 March 2018; published 11 July 2018)

We theoretically investigate pumping of phonons by the dynamics of a magnetic film into a nonmagnetic contact. The enhanced damping due to the loss of energy and angular momentum shows interference patterns as a function of the resonance frequency and magnetic film thickness that cannot be described by viscous ("Gilbert") damping. The phonon pumping depends on the magnetization direction as well as geometrical and material parameters and is observable, e.g., in thin films of yttrium iron garnet on a thick dielectric substrate.

DOI: 10.1103/PhysRevLett.121.027202

The dynamics of ferromagnetic heterostructures is at the root of devices for information and communication technologies [1–5]. When a normal metal contact is attached to a ferromagnet, the magnetization dynamics drives a spin current through the interface. This effect is known as spin pumping and can strongly enhance the (Gilbert) viscous damping in ultrathin magnetic films [6–8]. Spin pumping and its (Onsager) reciprocal, the spin transfer torque [9,10], are crucial in spintronics, as they allow electric control and detection of magnetization dynamics. When a magnet is connected to a nonmagnetic insulator instead of a metal, angular momentum cannot leave the magnet in the form of electronic or magnonic spin currents, but it can do so in the form of phonons. Half a century ago, it was reported [11,12] and explained [13–16] that magnetization dynamics can generate phonons by magnetostriction. More recently, the inverse effect of magnetization dynamics excited by surface acoustic waves (SAWs) has been studied [17–20] and found to generate spin currents in proximity normal metals [21,22]. The emission and detection of SAWs were combined in one and the same device [23,24], and an adiabatic transformation between magnons and phonons was observed in inhomogeneous magnetic fields [25]. The angular momentum of phonons [26,27] has recently come into focus again in the context of the Einstein–de Haas effect [28] and spin-phonon interactions, in general [29]. The interpretation of the phonon angular momentum in terms of orbital and spin contributions [29] has been challenged [30], a discussion that bears similarities with the interpretation of the photon angular momentum [31]. In our opinion, this distinction is rather semantic, since it is not required to arrive at concrete results. A recent quantum theory of the dynamics of a magnetic impurity [32] predicts a broadening of the electron spin resonance and a renormalized g factor by coupling to an elastic continuum via the spin-orbit interaction, which appears to be related to the enhanced damping and effective gyromagnetic ratio discussed here.

A phonon current generated by magnetization dynamics generates damping by carrying away angular momentum and energy from the ferromagnet. While the phonon contribution to the bulk Gilbert damping has been studied theoretically [33–38], the damping enhancement by interfaces to nonmagnetic substrates or overlayers has to our knowledge not been addressed before. Here we present a theory of the coupled lattice and magnetization dynamics of a ferromagnetic film attached to a half-infinite nonmagnet, which serves as an ideal phonon sink. We predict, for instance, significantly enhanced damping when an yttrium iron garnet (YIG) film is grown on a thick gadolinium gallium garnet (GGG) substrate.

We consider an easy-axis magnetic film with a static external magnetic field and equilibrium magnetization either normal (see Fig. 1) or parallel to the plane. The magnet is connected to a semi-infinite elastic material. The magnetization and lattice are coupled by the magnetocrystalline anisotropy and the magnetoelastic interaction, giving rise to coupled field equations of motion in the magnet [39–42]. By matching these with the lattice dynamics in the nonmagnet by proper boundary conditions, we predict the dynamics of the heterostructure as a function of geometrical and constitutive parameters. We find that

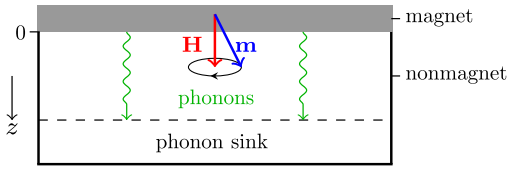

FIG. 1. Magnetic film (shaded) with magnetization **m** attached to a semi-infinite elastic material, which serves as an ideal phonon sink.

 © 2018 American Physical Society

magnetization dynamics induced, e.g., by ferromagnetic resonance (FMR) excites the lattice in the attached nonmagnet. In analogy with the electronic case, we call this effect "phonon pumping" that affects the magnetization dynamics. We consider only equilibrium magnetizations that are normal or parallel to the interface, in which the pumped phonons are pure shear waves that carry angular momentum. We note that for general magnetization directions both shear and pressure waves are emitted, however.

We consider a magnetic film (metallic or insulating) that extends from $z = -d$ to $z = 0$. It is subject to sufficiently high magnetic fields H_0 such that magnetization is uniform, i.e., $\mathbf{M}(\mathbf{r}) = \mathbf{M}$. For in-plane magnetizations, $H_0 > M_s$, where the magnetization M_s governs the demagnetizing field [43]. The energy of the magnet-nonmagnet bilayer can be written

$$E = E_T + E_{\rm el} + E_Z + E_D + E_K^0 + E_{\rm me}, \tag{1}$$

which are integrals over the energy densities $\varepsilon_X(\mathbf{r})$. The different contributions are explained in the following.

The kinetic energy density of the elastic motion reads

$$\varepsilon_T(\mathbf{r}) = \begin{cases} \frac{1}{2}\rho\dot{\mathbf{u}}^2(\mathbf{r}), & z > 0, \\ \frac{1}{2}\tilde{\rho}\dot{\mathbf{u}}^2(\mathbf{r}), & -d < z < 0, \end{cases} \tag{2}$$

and the elastic energy density [44]

$$\varepsilon_{\rm el} = \begin{cases} \frac{1}{2}\lambda[\sum_\alpha X_{\alpha\alpha}(\mathbf{r})]^2 + \mu\sum_{\alpha\beta} X_{\alpha\beta}^2(\mathbf{r}), & z > 0, \\ \frac{1}{2}\tilde{\lambda}[\sum_\alpha X_{\alpha\alpha}(\mathbf{r})]^2 + \tilde{\mu}\sum_{\alpha\beta} X_{\alpha\beta}^2(\mathbf{r}), & -d < z < 0, \end{cases} \tag{3}$$

where $\alpha, \beta \in \{x, y, z\}$, λ and μ are the Lamé parameters, and ρ is the mass density of the nonmagnet. The tilded parameters are those of the magnet. The strain tensor $X_{\alpha\beta}$ is defined in terms of the displacement fields $u_\alpha(\mathbf{r})$:

$$X_{\alpha\beta}(\mathbf{r}) = \frac{1}{2}\left(\frac{\partial u_\alpha(\mathbf{r})}{\partial r_\beta} + \frac{\partial u_\beta(\mathbf{r})}{\partial r_\alpha}\right). \tag{4}$$

$E_Z = -\mu_0 V \mathbf{M}\cdot\mathbf{H}_{\rm ext}$ is the Zeeman energy for $\mathbf{H}_{\rm ext} = \mathbf{H}_0 + \mathbf{h}(t)$, where $\mathbf{h}(t)$ is time dependent. $E_D = \frac{1}{2}\mu_0 V \mathbf{M}^T \mathcal{D}\mathbf{M}$ is the magnetostatic energy with shape-dependent demagnetization tensor $\mathcal{D}$ and V the volume of the magnet. For a thin film with the z axis along the surface normal $\mathbf{n}_0$, $\mathcal{D}_{zz} = 1$, while the other components vanish. $E_K^0 = K_1 V(\mathbf{m}\times\mathbf{n}_0)^2$ is the uniaxial magnetocrystalline anisotropy in the absence of lattice deformations, where $\mathbf{m} = \mathbf{M}/M_s$ and K_1 is the anisotropy constant. The magnetoelastic energy $E_{\rm me}$ couples the magnetization to the lattice, as discussed in the following.

The magnetoelastic energy density can be expanded as

$$\varepsilon_{\rm me}(\mathbf{r}) = \frac{1}{M_s^2}\sum_{\alpha,\beta} M_\alpha(\mathbf{r}) M_\beta(\mathbf{r}) \times [B_{\alpha\beta} X_{\alpha\beta}(\mathbf{r}) + C_{\alpha\beta}\Omega_{\alpha\beta}(\mathbf{r})]. \tag{5}$$

For an isotropic medium, the magnetoelastic constants $B_{\alpha\beta}$ read [45]

$$B_{\alpha\beta} = \delta_{\alpha\beta} B_\parallel + (1 - \delta_{\alpha\beta}) B_\perp. \tag{6}$$

Rotational deformations as expressed by the tensor

$$\Omega_{\alpha\beta}(\mathbf{r}) = \frac{1}{2}\left(\frac{\partial u_\alpha(\mathbf{r})}{\partial r_\beta} - \frac{\partial u_\beta(\mathbf{r})}{\partial r_\alpha}\right) \tag{7}$$

are often disregarded [39–42,46] but lead to a position dependence of the easy axis $\mathbf{n}(\mathbf{r})$ from the equilibrium value $\mathbf{n}_0 = \mathbf{e}_z$ and an anisotropy energy density [29,47,48]

$$\varepsilon_K(\mathbf{r}) = \frac{K_1}{M_s^2}[\mathbf{M}\times\mathbf{n}(\mathbf{r})]^2. \tag{8}$$

To first order in the small deformation,

$$\delta\mathbf{n}(\mathbf{r}) = \mathbf{n}(\mathbf{r}) - \mathbf{n}_0 = \begin{pmatrix} \Omega_{xz}(\mathbf{r}) \\ \Omega_{yz}(\mathbf{r}) \\ 0 \end{pmatrix}, \tag{9}$$

$$\varepsilon_K(\mathbf{r}) = \varepsilon_K^0 + 2K_1(\mathbf{n}_0 - m_z\mathbf{m})\cdot\delta\mathbf{n}(\mathbf{r}). \tag{10}$$

From $\Omega_{\alpha\beta} = -\Omega_{\beta\alpha}$, it follows that (for nonchiral crystal structures) $C_{\alpha\beta} = -C_{\beta\alpha}$. For the uniaxial anisotropy considered here, $C_{xz} = C_{yz} = -K_1$. The magnetoelastic coupling due to the magnetocrystalline anisotropy thus contributes [47]

$$\varepsilon_{\rm me}^K(\mathbf{r}) = -\frac{2K_1}{M_s^2} M_z(\mathbf{r})[M_x(\mathbf{r})\Omega_{xz}(\mathbf{r}) + M_y(\mathbf{r})\Omega_{yz}(\mathbf{r})]. \tag{11}$$

Pure YIG is magnetically very soft, so the magnetoelastic constants are much larger than the anisotropy constant [49,50]:

$$B_\parallel = 3.48\times10^5\ \mathrm{J\times m^{-3}}, \qquad B_\perp = 6.96\times10^5\ \mathrm{J\times m^{-3}}, \qquad K_1 = -6.10\times10^2\ \mathrm{J\times m^{-3}}, \tag{12}$$

but this ratio can be very different for other magnets. We find below that for the Kittel mode dynamics both coupling processes cannot be distinguished, even though they can characteristically affect the magnon-phonon coupling for finite wave numbers.

The magnetization dynamics within the magnetic film is described by the Landau-Lifshitz-Gilbert (LLG) equation [51,52]

$$\dot{\mathbf{m}} = -\gamma\mu_0 \mathbf{m} \times \mathbf{H}_{\text{eff}} + \boldsymbol{\tau}_m^{(\alpha)}, \tag{13}$$

where $-\gamma$ is the gyromagnetic ratio, the effective magnetic field which includes the magnetoelastic coupling

$$\mathbf{H}_{\text{eff}} = -\boldsymbol{\nabla}_{\mathbf{m}} E/(\mu_0 V M_s), \tag{14}$$

and the Gilbert damping torque [52]

$$\boldsymbol{\tau}_m^{(\alpha)} = \alpha \mathbf{m} \times \dot{\mathbf{m}}. \tag{15}$$

The equation of motion of the elastic continuum reads [44]

$$\ddot{\mathbf{u}}(\mathbf{r}, t) = c_t^2 \triangle \mathbf{u}(\mathbf{r}, t) + (c_l^2 - c_t^2)\boldsymbol{\nabla}[\boldsymbol{\nabla} \cdot \mathbf{u}(\mathbf{r}, t)], \tag{16}$$

with longitudinal and transverse sound velocities

$$c_l = \sqrt{\frac{\lambda + 2\mu}{\rho}} \quad \text{and} \quad c_t = \sqrt{\frac{\mu}{\rho}}, \tag{17}$$

respectively, where elastic constants and the mass density of the nonmagnet and magnet can differ.

A uniform precession of the magnetization interacts with the lattice deformation at the surfaces of the magnetic film [13,14] and at defects in the bulk. The present theory then holds when the thickness of the magnetic film $d \ll \sqrt{A}$, where A is the cross section area. The Kittel mode induces lattice distortions that are uniform in the film plane $u_\alpha(\mathbf{r}) = u_\alpha(z)$ [14]. The elastic energy density is then affected by shear waves only:

$$\varepsilon_{\text{el}}(z) = \begin{cases} \frac{\mu}{2}[u_x'^2(z) + u_y'^2(z)], & z > 0, \\ \frac{\tilde{\mu}}{2}[u_x'^2(z) + u_y'^2(z)], & -d < z < 0, \end{cases} \tag{18}$$

where $u_\alpha'(z) = \partial u_\alpha(z)/\partial z$. The magnetic field $\mathbf{H}_{\text{ext}} = (h_x(t), h_y(t), H_0)^T$ with monochromatic drive $h_{x,y}(t) = \text{Re}(h_{x,y} e^{-i\omega t})$ and static component H_0 along the z axis. At the FMR frequency, $\omega_\perp = \omega_H + \omega_A$ with $\omega_H = \gamma\mu_0 H_0$ and $\omega_A = \gamma(2K_1/M_s - \gamma\mu M_s)$. The equilibrium magnetization is perpendicular for $\omega_\perp > 0$. The magnetoelastic energy derived above then simplifies to

$$E_{\text{me}}^z = \frac{(B_\perp - K_1)A}{M_s} \sum_{\alpha=x,y} M_\alpha [u_\alpha(0) - u_\alpha(-d)], \tag{19}$$

which results in surface shear forces $F_\pm(0) = -F_\pm(-d) = -(B_\perp - K_1)A m_\pm$, with $F_\pm = F_x \pm iF_y$. These forces generate a stress or transverse momentum current in the z direction (see Supplemental Material [53]):

$$j_\pm(z) = -\mu(z) u_\pm'(z), \tag{20}$$

with $\mu(z) = \mu$ for $z > 0$, $\mu(z) = \tilde{\mu}$ for $-d < z < 0$, and $u_\pm = u_x \pm iu_y$, which is related to the transverse momentum $p_\pm(z) = \rho[\dot{u}_x(z) \pm i\dot{u}_y(z)]$ by Newton's equation:

$$\dot{p}_\pm(z) = -\frac{\partial}{\partial z} j_\pm(z). \tag{21}$$

The boundary conditions require momentum conservation and elastic continuity at the interfaces:

$$j_\pm(-d) = (B_\perp - K_1) m_\pm, \tag{22}$$

$$j_\pm(0^+) - j_\pm(0^-) = -(B_\perp - K_1) m_\pm, \tag{23}$$

$$u_\pm(0^+) = u_\pm(0^-). \tag{24}$$

We treat the magnetoelastic coupling as a small perturbation, and therefore we approximate the magnetization $m_\pm$ entering the above boundary conditions as independent of the lattice displacement $u_\pm$. The loss of angular momentum (see Supplemental Material [53]) affects the magnetization dynamics in the LLG equation in the form of a torque, which we derive from the magnetoelastic energy (19):

$$\begin{aligned} \dot{m}_\pm|_{\text{me}} &= \pm i \frac{\omega_c}{d}[u_\pm(0) - u_\pm(-d)] \\ &= \pm i\omega_c \text{Re}(v) m_\pm \mp \omega_c \text{Im}(v) m_\pm, \end{aligned} \tag{25}$$

where $\omega_c = \gamma(B_\perp - K_1)/M_s$ (for YIG, $\omega_c = 8.76 \times 10^{11}\ \text{s}^{-1}$) and $v = [u_\pm(0) - u_\pm(-d)]/(dm_\pm)$. We can distinguish an effective field

$$\mathbf{H}_{\text{me}} = \frac{\omega_c}{\gamma\mu_0} \text{Re}(v) \mathbf{e}_z \tag{26}$$

and a damping coefficient

$$\alpha_{\text{me}}^{(\perp)} = -\frac{\omega_c}{\omega} \text{Im} v. \tag{27}$$

The latter can be compared with the Gilbert damping constant α that enters the linearized equation of motion as

$$\dot{m}_\pm|_\alpha = \pm i\alpha\dot{m}_\pm = \pm\alpha\omega m_\pm. \tag{28}$$

With the ansatz

$$u_\pm(z,t) = \begin{cases} C_\pm e^{ikz - i\omega t}, & z > 0, \\ D_\pm e^{i\tilde{k}z - i\omega t} + E_\pm e^{-i\tilde{k}z - i\omega t}, & -d < z < 0, \end{cases} \tag{29}$$

we obtain

$$v = \frac{M_s \omega_c}{\omega \gamma d \tilde{\rho} \tilde{c}_t} \frac{2[\cos(\tilde{k}d) - 1] - i\frac{\rho c_t}{\tilde{\rho}\tilde{c}_t}\sin(\tilde{k}d)}{\sin(\tilde{k}d) + i\frac{\rho c_t}{\tilde{\rho}\tilde{c}_t}\cos(\tilde{k}d)}, \quad (30)$$

and the damping coefficient for perpendicular magnetization

$$\alpha_{\mathrm{me}}^{(\perp)} = \left(\frac{\omega_c}{\omega}\right)^2 \frac{M_s}{\gamma d \tilde{\rho}\tilde{c}_t} \frac{\rho c_t}{\tilde{\rho}\tilde{c}_t} \frac{4\sin^4(\frac{\tilde{k}d}{2})}{\sin^2(\tilde{k}d) + (\frac{\rho c_t}{\tilde{\rho}\tilde{c}_t})^2 \cos^2(\tilde{k}d)}, \quad (31)$$

where $\omega = c_t k = \tilde{c}_t \tilde{k}$. The oscillatory behavior of the damping $\alpha_{\mathrm{me}}^{(\perp)}$ comes from the interference of the elastic waves that are generated at the top and bottom surfaces of the magnetic film. When they constructively (destructively) interfere at the FMR frequency, the damping is enhanced (suppressed), because the magnon-phonon coupling and phonon emission are large (small).

When $\rho c_t \ll \tilde{\rho}\tilde{c}_t$ (soft substrate) or when acoustic impedances are matched ($\rho c_t = \tilde{\rho}\tilde{c}_t$), damping at the resonance $\tilde{k}d = (2n+1)\pi$ with $n \in \mathbb{N}_0$ [14] simplifies to

$$\alpha_{\mathrm{me}}^{(\perp)} \to \left(\frac{\omega_c}{\omega}\right)^2 \frac{4M_s}{\gamma d \rho c_t}. \quad (32)$$

When $\rho c_t \gg \tilde{\rho}\tilde{c}_t$ (hard substrate), the magnet is acoustically pinned at the interface and the acoustic resonances are at $\tilde{k}d = (2n+1)\pi/2$ [14] with

$$\alpha_{\mathrm{me}}^{(\perp)} \to \left(\frac{\omega_c}{\omega}\right)^2 \frac{M_s}{\gamma d \tilde{\rho}\tilde{c}_t} \frac{\rho c_t}{\tilde{\rho}\tilde{c}_t}. \quad (33)$$

In contrast to Gilbert damping, $\alpha_{\mathrm{me}}^{(\perp)}$ depends on the frequency and vanishes in the limits $\omega \to 0$ and $\omega \to \infty$. Therefore, it does not obey the LLG phenomenology and in the nonlinear regime does not simply enhance α in Eq. (15). The magnetization damping α_0 in bulk magnetic insulators, on the other hand, is usually of the Gilbert type. It is caused by phonons, as well, but not necessarily the magnetoelastic coupling. A theory of Gilbert damping [38] assumes a bottleneck process by sound wave attenuation, which appears realistic for magnets with high acoustic quality such as YIG. In the present phonon-pumping model, energy and angular momentum is lost by the emission of sound waves into an attached perfect phonon wave guide, so the pumping process dominates. Such a scenario could also dominate the damping in magnets in which the magnetic quality is relatively higher than the acoustic one.

When the field is rotated to $\mathbf{H}_{\mathrm{ext}} = (h_x(t), H_0, h_z(t))^T$, the equilibrium magnetization is in the in-plane y direction and the magnetoelastic energy couples only to the strain u_y:

$$E_{\mathrm{me}}^{y} = \frac{(B_\perp - K_1)A}{M_s} M_z [u_y(0) - u_y(-d)]. \quad (34)$$

The FMR frequency for in-plane magnetization $\omega_\parallel = \omega_H \sqrt{1 - \omega_A/\omega_H}$ with $\omega_A < \omega_H$. The magnetoelastic coupling generates again only transverse sound waves. The linearized LLG equation including the phononic torques reads now

$$\dot{m}_x = (\omega_H + \omega_{\mathrm{me}}) m_z - \gamma\mu_0 h_z - \omega_A m_z + (\alpha + \alpha_{\mathrm{me}})\dot{m}_z, \quad (35)$$

$$\dot{m}_z = -\omega_H m_x + \gamma\mu_0 h_x - \alpha \dot{m}_x, \quad (36)$$

where α_{me} is given by Eq. (27) and $\omega_{\mathrm{me}} = \gamma\mu_0 H_{\mathrm{me}}$ with effective field $H_{\mathrm{me}} = \mathbf{H}_{\mathrm{me}} \cdot \mathbf{e}_z$ given by Eq. (26). Both H_{me} and α_{me} contribute only to $\dot{m}_x$. The phonon pumping is always less efficient for the in-plane configuration:

$$\alpha_{\mathrm{me}}^{(\parallel)} = \frac{1}{1 + (\omega_\parallel/\omega_H)^2} \alpha_{\mathrm{me}}^{(\perp)}. \quad (37)$$

As an example, we insert parameters for a thin YIG film on a semi-infinite GGG substrate at room temperature. We have chosen YIG because of its low intrinsic damping and high-quality interface to the GGG substrate. Substantially larger magnetoelastic coupling in other materials should be offset against generally larger bulk damping. For GGG, $\rho = 7.07 \times 10^3$ kg $\times$ m^{-3}, $c_l = 6411$ m$\times$ s^{-1}, and $c_t = 3568$ m$\times$ s^{-1} [55]. For YIG, $M_s = 1.4 \times 10^5$ A$\times$ m^{-1}, $\gamma = 1.76 \times 10^{11}$ s^{-1} T^{-1}, $\tilde{\rho} = 5170$ kg $\times$ m^{-3}, $\tilde{c}_l = 7209$ m$\times$ s^{-1}, $\tilde{c}_t = 3843$ m$\times$ s^{-1}, and $\omega_c = 8.76 \times 10^{11}$ s^{-1} [49,50]. The ratio of the acoustic impedances $\tilde{\rho}\tilde{c}_t/\rho c_t = 0.79$. The damping enhancement $\alpha_{\mathrm{me}}^{(\perp)}$ is shown in Fig. 2 over a range of FMR frequencies and film thicknesses. The FMR frequencies $\omega_\perp = \omega_H + \omega_A$ and $\omega_\parallel = \omega_H\sqrt{1 - \omega_A/\omega_H}$ for the normal and in-plane configurations are tunable by the static magnetic field component H_0 via $\omega_H = \gamma\mu_0 H_0$. The damping enhancement peaks at acoustic resonance frequencies $\nu \approx n\tilde{c}_t/(2d)$. The counterintuitive result that the damping increases for thicker films can be understood by the competition between

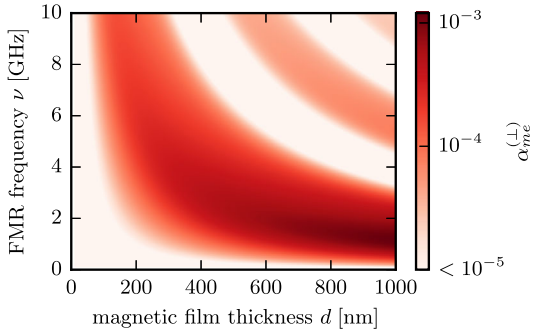

FIG. 2. Damping enhancement $\alpha_{\mathrm{me}}^{(\perp)}$ by phonon pumping in a YIG film on a semi-infinite GGG substrate, as given by Eq. (31).

the magnetoelastic effect that increases with thickness at the resonances and wins against the increase in total magnetization. However, with increasing thickness, the resonance frequencies decrease below a minimum value at which FMR can be excited. For a fixed FMR frequency, $\alpha_{\rm me} \to 0$ for $d \to \infty$. For comparison, the Gilbert damping in nanometer-thin YIG films is of the order of $\alpha \sim 10^{-4}$ [56], which is larger than corresponding values for single crystals. We conclude that the enhanced damping is at least partly caused by an interaction with the substrate and not by a reduced crystal quality.

The resonances in the figures are very broad, because the $\rho c_t \approx \tilde{\rho}\tilde{c}_t$ implies a very strong coupling of the discrete phonons in the thin magnetic layer with the phonon continuum in the substrate. When an acoustic mismatch is introduced, the broad peaks increasingly sharpen, reflecting the increased lifetime of the magnon polaron resonances in the magnet.

The frequency-dependent effective magnetic field $H_{\rm me}^{(\perp)}$ is shown in Fig. 3. The frequency dependence of $H_{\rm me}^{(\perp)}$ implies a weak frequency dependence of the effective gyromagnetic ratio

$$\gamma_{\rm eff}^{(\perp)} = \gamma\left(1 + \frac{\gamma\mu_0 H_{\rm me}^{(\perp)}}{\omega}\right). \tag{38}$$

In the limit of vanishing film thickness, $\mu_0 H_{\rm me}^{(\perp)} \to -(B_\perp - K_1)^2/(M_s\tilde{\mu})$.

We assumed that the nonmagnet is an ideal phonon sink, which means that injected sound waves do not return. In the opposite limit in which the phonons cannot escape, i.e., when the substrate is a thin film with high acoustic quality, the additional damping vanishes. This can be interpreted in terms of a phonon accumulation that, when allowed to thermalize, generates a phonon chemical potential and/or nonequilibrium temperature. The nonequilibrium thermodynamics of phonons in magnetic nanostructures is a subject of our ongoing research.

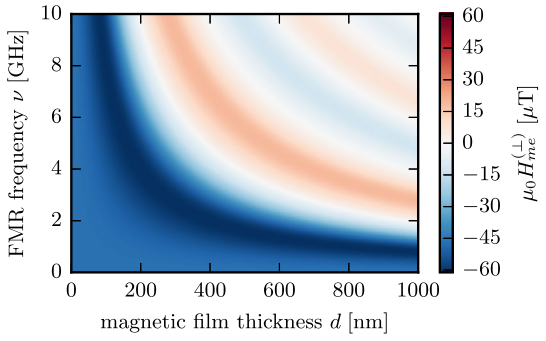

FIG. 3. Effective field $H_{\rm me}^{(\perp)}$ generated by the magnetoelastic generation of phonons in a YIG film on a semi-infinite GGG substrate, as given by Eq. (26).

The damping enhancement by phonons may be compared with that from electronic spin pumping [6–8]:

$$\alpha_{\rm sp} = \frac{\gamma\hbar}{4\pi d M_s}\frac{h}{e^2}g, \tag{39}$$

which is inversely proportional to the thickness d of the magnetic film and does not depend on the FMR frequency, i.e., obeys the LLG phenomenology. Here, g is the spin mixing conductance per unit area at the interface. While phonons can be pumped into any elastic material, spin pumping requires an electrically conducting contact. With a typical value of $hg/e^2 \sim 10^{18}$ m^{-2}, the damping enhancement of YIG on platinum is $\alpha_{\rm sp} \sim 10^{-2}$ nm$/d$. The physics is quite different, however, since $\alpha_{\rm sp}$, in contrast to $\alpha_{\rm me}$, does not require coherence over the interface.

In conclusion, the pumping of phonons by magnetic anisotropy and magnetostriction causes frequency-dependent contributions to the damping and effective field of the magnetization dynamics. The generation of phonons by magnetic precession can cause significant damping in a magnetic film when grown on an insulating, nonmagnetic substrate and partly explains the increased damping invariably observed for thinner films. The implications of further reaching ramifications, such as phonon-induced dynamic exchange interactions, phonon accumulations, and the phonon spin Seebeck effect require additional research.

This work is financially supported by the Nederlandse Organisatie voor Wetenschappelijk Onderzoek (NWO) as well as by the Grant-in-Aid for Scientific Research on Innovative Area, "Nano Spin Conversion Science" (Grant No. 26103006). H. K. acknowledges support from the Iran Science Elites Federation. We acknowledge useful discussions with Yaroslav Blanter, Rembert Duine, Akashdeep Kamra, Eiji Saitoh, and Sanchar Sharma.

[1] S. Bader and S. Parkin, Annu. Rev. Condens. Matter Phys. **1**, 71 (2010).
[2] V. V. Kruglyak, S. O. Demokritov, and D. Grundler, J. Phys. D **43**, 264001 (2010).
[3] F. Pulizzi, Nat. Mater. **11**, 367 (2012).
[4] A. V. Chumak, V. I. Vasyuchka, A. A. Serga, and B. Hillebrands, Nat. Phys. **11**, 453 (2015).
[5] S. A. Nikitov, D. V. Kalyabin, I. V. Lisenkov, A. Slavin, Y. N. Barabanenkov, S. A. Osokin, A. V. Sadovnikov, E. N. Beginin, M. A. Morozova, Y. A. Filimonov, Y. V. Khivintsev, S. L. Vysotsky, V. K. Sakharov, and E. S. Pavlov, Phys. Usp. **58**, 1002 (2015).
[6] Y. Tserkovnyak, A. Brataas, and G. E. W. Bauer, Phys. Rev. Lett. **88**, 117601 (2002).
[7] Y. Tserkovnyak, A. Brataas, G. E. W. Bauer, and B. I. Halperin, Rev. Mod. Phys. **77**, 1375 (2005).
[8] A. Kapelrud and A. Brataas, Phys. Rev. Lett. **111**, 097602 (2013).
[9] L. Berger, Phys. Rev. B **54**, 9353 (1996).

[10] J. Slonczewski, J. Magn. Magn. Mater. **159**, L1 (1996).
[11] H. Bömmel and K. Dransfeld, Phys. Rev. Lett. **3**, 83 (1959).
[12] M. Pomerantz, Phys. Rev. Lett. **7**, 312 (1961).
[13] R. L. Comstock and R. C. LeCraw, J. Appl. Phys. **34**, 3022 (1963).
[14] M. H. Seavey, Proc. IEEE **53**, 1387 (1965).
[15] T. Kobayashi, R. Barker, and A. Yelon, IEEE Trans. Magn. **7**, 755 (1971).
[16] T. Kobayashi, R. Barker, and A. Yelon, IEEE Trans. Magn. **8**, 382 (1972).
[17] M. Weiler, L. Dreher, C. Heeg, H. Huebl, R. Gross, M. S. Brandt, and S. T. B. Goennenwein, Phys. Rev. Lett. **106**, 117601 (2011).
[18] L. Dreher, M. Weiler, M. Pernpeintner, H. Huebl, R. Gross, M. S. Brandt, and S. T. B. Goennenwein, Phys. Rev. B **86**, 134415 (2012).
[19] P. G. Gowtham, T. Moriyama, D. C. Ralph, and R. A. Buhrman, J. Appl. Phys. **118**, 233910 (2015).
[20] X. Li, D. Labanowski, S. Salahuddin, and C. S. Lynch, J. Appl. Phys. **122**, 043904 (2017).
[21] K. Uchida, T. An, Y. Kajiwara, M. Toda, and E. Saitoh, Appl. Phys. Lett. **99**, 212501 (2011).
[22] M. Weiler, H. Huebl, F. S. Goerg, F. D. Czeschka, R. Gross, and S. T. B. Goennenwein, Phys. Rev. Lett. **108**, 176601 (2012).
[23] S. Bhuktare, A. Bose, H. Singh, and A. A. Tulapurkar, Sci. Rep. **7**, 840 (2017).
[24] S. Bhuktare, H. Singh, A. Bose, and A. A. Tulapurkar, arXiv:1712.02711.
[25] J. Holanda, D. S. Maior, A. Azevedo, and S. M. Rezende, Nat. Phys. **14**, 500 (2018).
[26] A. T. Levine, Nuovo Cimento **26**, 190 (1962).
[27] A. G. McLellan, J. Phys. C **21**, 1177 (1988).
[28] L. Zhang and Q. Niu, Phys. Rev. Lett. **112**, 085503 (2014).
[29] D. A. Garanin and E. M. Chudnovsky, Phys. Rev. B **92**, 024421 (2015).
[30] S. C. Tiwari, arXiv:1708.07407.
[31] E. Leader, Phys. Lett. B **756**, 303 (2016).
[32] J. H. Mentink, M. I. Katsnelson, and M. Lemeshko, arXiv:1802.01638.
[33] T. Kobayashi, R. C. Barker, and A. Yelon, J. Phys. (Paris), Colloq. **32**, C1 (1971).
[34] T. Kobayashi, R. C. Barker, J. L. Bleustein, and A. Yelon, Phys. Rev. B **7**, 3273 (1973).
[35] T. Kobayashi, R. C. Barker, and A. Yelon, Phys. Rev. B **7**, 3286 (1973).
[36] E. Rossi, O. G. Heinonen, and A. H. MacDonald, Phys. Rev. B **72**, 174412 (2005).
[37] A. Widom, C. Vittoria, and S. D. Yoon, J. Appl. Phys. **108**, 073924 (2010).
[38] C. Vittoria, S. D. Yoon, and A. Widom, Phys. Rev. B **81**, 014412 (2010).
[39] E. Abrahams and C. Kittel, Phys. Rev. **88**, 1200 (1952).
[40] C. Kittel and E. Abrahams, Rev. Mod. Phys. **25**, 233 (1953).
[41] C. Kittel, Phys. Rev. **110**, 836 (1958).
[42] M. I. Kaganov and V. M. Tsukernik, Sov. Phys. JETP **9**, 151 (1959).
[43] H. Knüpfer and C. B. Muratov, J. Nonlinear Sci. **21**, 921 (2011).
[44] L. D. Landau and E. M. Lifshitz, *Theory of Elasticity*, 2nd ed., Course in Theoretical Physics Vol. 7 (Pergamon, Oxford, 1970).
[45] A. Rückriegel, P. Kopietz, D. A. Bozhko, A. A. Serga, and B. Hillebrands, Phys. Rev. B **89**, 184413 (2014).
[46] C. Kittel, Rev. Mod. Phys. **21**, 541 (1949).
[47] D. A. Garanin and E. M. Chudnovsky, Phys. Rev. B **56**, 11102 (1997).
[48] R. Jaafar, E. M. Chudnovsky, and D. A. Garanin, Phys. Rev. B **79**, 104410 (2009).
[49] A. G. Gurevich and G. A. Melkov, *Magnetization Oscillations and Waves* (CRC, Boca Raton, FL, 1996).
[50] P. Hansen, J. Appl. Phys. **45**, 3638 (1974).
[51] L. D. Landau and E. Lifshitz, Phys. Z. Sowjetunion **8**, 153 (1935).
[52] T. L. Gilbert, IEEE Trans. Magn. **40**, 3443 (2004).
[53] See Supplemental Material at http://link.aps.org/supplemental/10.1103/PhysRevLett.121.027202 which includes Ref. [54], for technical details and additional derivations.
[54] E. B. Magrab, *Vibrations of Elastic Systems* (Springer, Dordrecht, 2012).
[55] Z. Kleszczewski and J. Bodzenta, Phys. Status Solidi B **146**, 467 (1988).
[56] H. Chang, P. Li, W. Zhang, T. Liu, A. Hoffmann, L. Deng, and M. Wu, IEEE Magn. Lett. **5**, 1 (2014).